PROPAGATION AND INTERFERENCE CHARACTERISTICS BY GROUP OF BUILDINGS IN MOBILE COMMUNICATION CHANNELS

Paul SELORMEY and Yasumitsu MIYAZAKI
Department of Information and Computer Sciences
Toyohashi University of Technology
Tempaku-cho, Toyohashi 441-8580, Japan
E-mail miyazaki@emlab.tutics.tut.ac.jp

1 Introduction

Wide-band digital indoor and future mobile communication systems are being developed in the quasi-millimeter and millimeter wave frequency bands. In such high-speed systems, the degradation of transmission quality by multipath fading constitutes a limiting barrier [1].

Multipath fading, which results from reflection, refraction and scattering of radio waves by buildings and other structures, gives rise to more than one path reaching the receiver and produces a distorted version of the transmitted signal. In mobile and indoor communication systems it cannot be eliminated, therefore multipath channel must be well characterized in order to reduce its effect in the design of such systems [2].

The objective of this research is to study the multipath fading and delay spread effects due to buildings in urban propagation channel. In particular, the effects of the building materials, shapes and number of buildings on multipath fading are being studied.

2 Channel Simulation Methods

Until recently, most reported results use the impulse-response method of modeling, and by this a computer simulation of a model, obtained through measurement, is designed with the purpose of predicting the response of the channel to any transmitted signal.

The modeling method based on the 3-dimensional UTD [3], is also receiving much attention. This method is known to be very accurate at high frequencies, and requires less computer resources compared with the FDTD method. However, there are several limitations of these methods as outlined in [4].

For our simulation, we used the FDTD [4, 5] total field formulation, and by the Yee's notations the FDTD difference equations are given as follows:

For free space,

$$\begin{aligned} E_z^{n+1}(i,j) &= E_z^n(i,j) + \frac{\Delta t}{\varepsilon_0 \Delta x}[H_y^{n+1/2}(i,j) - H_y^{n+1/2}(i-1,j)] \\ &\quad - \frac{\Delta t}{\varepsilon_0 \Delta y}[H_x^{n+1/2}(i,j) - H_x^{n+1/2}(i,j-1)] - \frac{\Delta t}{\varepsilon_0} J_z^{n+1/2} \end{aligned} \tag{1}$$

On a perfect conductor,

$$E_z^n(i,j) = -E_z^n(i,j) \tag{2}$$

In dielectric material (buildings),

$$\begin{aligned} E_z^{n+1}(i,j) &= E_z^n(i,j) + \frac{\Delta t}{\varepsilon \Delta x}[H_y^{n+1/2}(i,j) - H_y^{n+1/2}(i-1,j)] \\ &\quad - \frac{\Delta t}{\varepsilon \Delta y}[H_x^{n+1/2}(i,j) - H_x^{n+1/2}(i,j-1)] - \frac{\Delta t}{\varepsilon} J_z^{n+1/2} \end{aligned} \tag{3}$$

where Δx, Δy, and Δt are the increments in x, y directions and time t, respectively.

of Fig. 3 is exterior part or the remaining part when Region I is excluded. By the computer similations, it is observed that the signals at the receiver locations R14 and similar sites of Region I are not so strongly affected by the exterior region, Region II, for the concrete buildings. For the perfect conductor buildings, there is a significant difference in the received signals at the location R14, as shown in Fig. 7. It could be concluded that the increased number of buildings has no or negligible effect on the received signals in concrete buildings channel.

Finally, for the Model A, the signal propagation patterns in the problem space after a total of 188.5 ns for both Cases 1 and 2 are shown in Figs. 8 and 9, respectively, for concrete buildings. In general, the electric field patterns show high peaks near the building corners along the line of sight. These are mainly due to diffractions and to some extent reflections at the corner points, which in these cases increase the received signal intensity. In both cases, the transmitter is located at $Tx1$ (11.0m, 55.0m).

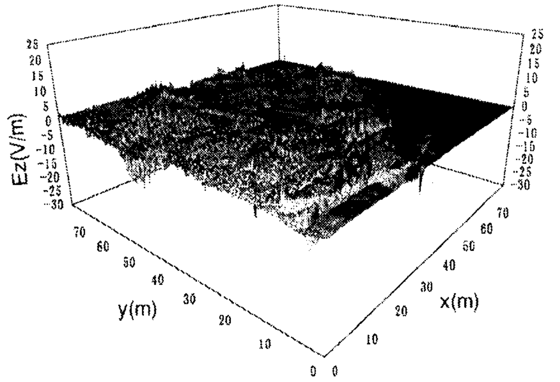

Fig. 8: Model A - Electric field patterns after 188.5 ns - Case 1.

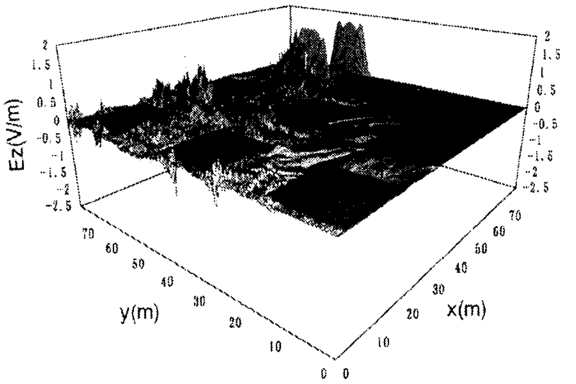

Fig. 9: Model A - Electric field patterns after 188.5 ns - Case 2.

5 Conclusion

With the FDTD method, it is becoming increasingly possible to simulate the outdoor radio wave propagation. The results have much more intuitive meaning than the impulse response and the UTD methods. Unlike the UTD and other methods very complex channels be well modeled. The main limitation is the two-dimensional approach as a result of the computer resources limitations. Therefore ground reflections, which are observed in practical situations, cannot be accounted for in this simulation. Also, the effect of antenna height on the radio wave propagation characteristics could not be investigated, and break point range, which defines a microcell size in LOS conditions along streets, could not be determined. However, with the 2D model enough information can still be obtained from the propagation channel. We can with great accuracy predict the wave propagation characteristics, that is, the field intensity decay and path loss distribution along the streets. When used together with the UTD method, very complex mobile communication environments can be completely modeled. Finally, the results will be compared with similar models using the UTD methods in both 2D and 3D.

References

[1] K. Uehara, Y. Takatori, K. Kagoshima; IEEE Trans. on Vech. Tech., vol. 48, p. 1511, 1999.

[2] H. Hashemi; Proc. of IEEE, vol. 81, p. 943, 1993.

[3] N. Papadakis, A. G. Kanatas, P. Constantinou; IEEE Trans. on Vech. Tech., vol. 47, p. 1012, 1998.

[4] P. Selormey, Y. Miyazaki; Proc. of IEICE General Conf., p. 1, Mar. 1997.

[5] Y. Miyazaki; 1996 Asia-Pacific MC Proc., vol. IV. p. 1333, 1996.

4 Numerical Results

The comparative results of the total received signals at the locations R3 and R8 for the Cases 1 and 2 are shown in Figs. 4 and 5. Plots for the Case 2 are shown in dotted lines. In both cases, the received signal at location R3 shows much variations with time, since it is an out of sight location. For each plot, the E-values are taken starting from time t = 0 therefore each plot shows an initial fast fading effect after which approximately regular patterns develop.

In the case of the LOS location R8, the initial signal received at the time $T_3 \simeq 138.2$ μs has the strongest power density. This is expected since the signal travels relatively a shorter distance. However, at the location R3, the initial signal received, at $T_8 \simeq 179.7$ μs, does not have the strongest power density. The reason is, R3 being OOS location, signals traveling to these locations are more reflected and absorbed. This effect is even better observed in the case of perfect conductor buildings.

At the location R8, the initial high signal is expectedly followed by a drastic decrease in the received power. However, due to the reflection of signal back into the main streets by the buildings, the received signals increased rapidly with some peak at approximately 380.0 μs.

Similar effects are observed at the locations R3. However, since location R3 is out of sight, the increase in received signals is gradual. In the case of the concrete buildings, very low signals are observed between 138 μs and 300 μs at the locations R8. It was observed that the initial signal is highly refracted and absorbed by the concrete buildings, resulting in the low received signal between 138 - 300 μs for location R8.

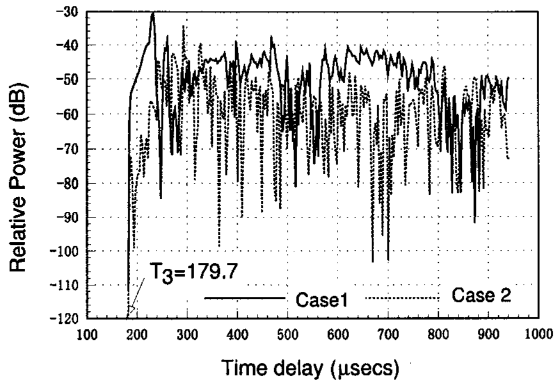

Fig. 4: Model A - Received signal at R3.

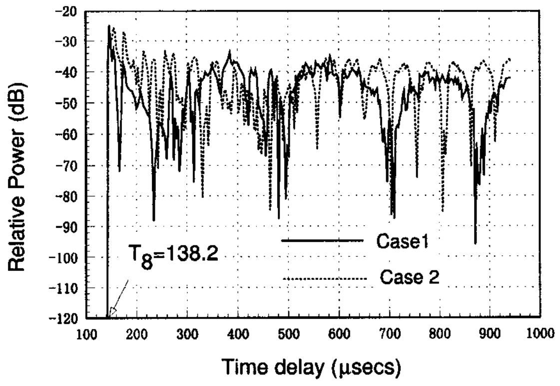

Fig. 5: Model A - Received signal at R8.

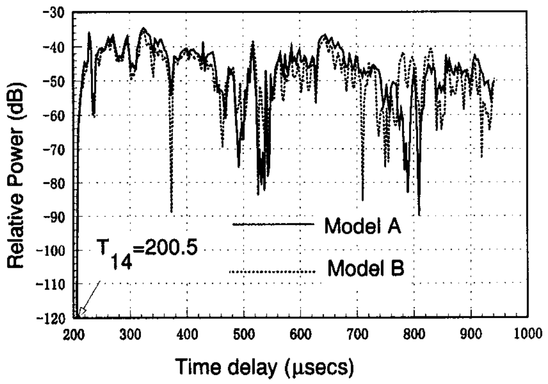

Fig. 6: Models A and B - Received electric signal at R14.

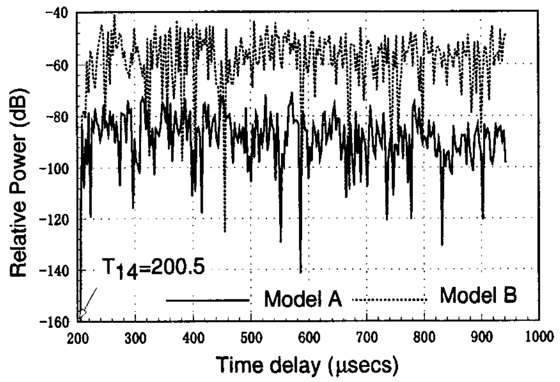

Fig. 7: Models A and B - Received electric signal at R14 (PEC).

In the Figs. 6 and 7, the comparative results of Models A and B are shown for the concrete and perfect conductor buildings, respectively. The Model B is partitioned into two regions, Regions I and II. Region I of the Fig. 3, corresponds to the Model A of Fig. 2, and Region II

The magnetic fields are given by the relations

$$H_y^{n+1/2}(i,j) = H_y^{n-1/2}(i,j) + \frac{\Delta t}{\mu_0 \Delta x}[E_z^n(i+1,j) - E_z^n(i,j)] \tag{4}$$

$$H_x^{n+1/2}(i,j) = H_x^{n-1/2}(i,j) + \frac{\Delta t}{\mu_0 \Delta y}[E_z^n(i,j+1) - E_z^n(i,j)] \tag{5}$$

For accuracy, cells size $\delta = \min(\Delta x,\, \Delta y)$ must be smaller than $\lambda/10$, where λ is the smallest wavelength in problem space. For stability, the time increment Δt is chosen to satisfy the Courant inequality. The Mur's absorption boundary condition is used to limit the simulation region. We assumed an antenna of point type at Tx in a street, vertical polarization and generates a line current of the following form, $\tau = 0.8$ μs being the pulse width,

$$J_z^{i,n} = J_{max}\cos(2\pi f t) \qquad |t| < \tau \tag{6}$$

where t is the time elapsed, J_{max} is the amplitude and f is the frequency of source.

Table 1: Simulation Parameters

Frequency of source, f	= 850 MHz
Cell Size, δ	= 0.02 m
Time Increment, Δt	= 37.7 ps
Relative Permittivity of Building	= 3.0
Conductivity of Building, σ	= 0.005 S/m
Current Amplitude, J_{max}	= 1000 A/m ^{2}
Pulse Width	= 0.8 μsecs

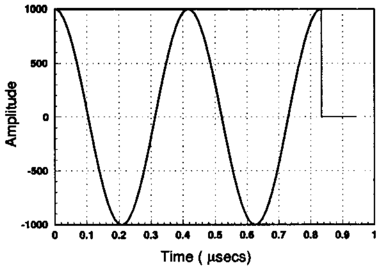

Fig. 1: Modulated signal in the time domain using BPSK.

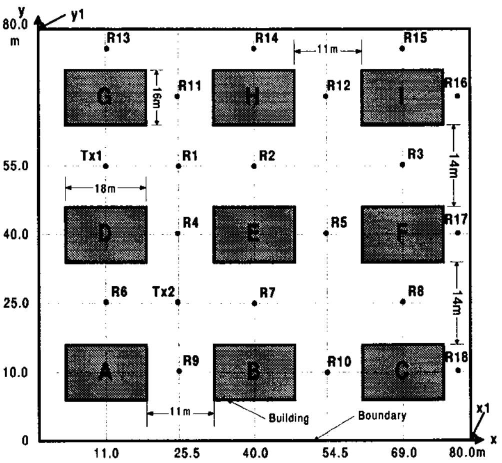

Fig. 2: Simulation model A.

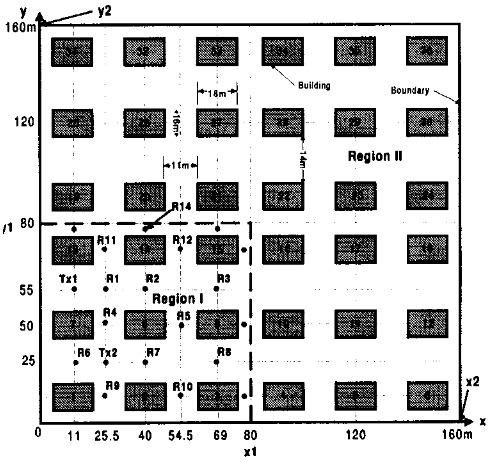

Fig. 3: Simulation model B.

3 Simulation Models

The Model A of 9 buildings, as shown in Fig. 2, is 80 × 80 m (or 4000 × 4000 in cell units). The Model B of 36 buildings, Fig. 3, is 160 × 160 m. For each model, two cases are considered. For Case 1, the building walls are made from concrete materials having relative permittivity of 3 and conductivity of 0.005 mho/m. The summary of the simulation parameters is given in Table 1. Also, for comparison, results are also presented for a Case 2, where the buildings are considered as made from perfect electric conductors (PEC).

For both models, $Tx1$ and $Tx2$ are transmitters locations, and results are presented for $Tx2$ at the location (25.5m, 25.0m). $R_i(i = 1, 2, ...18)$ are the receiver locations. In this paper, results are presented for the out of sight receiver locations R3(69.0m, 55.0m) and R14(40.0m, 79.0m), and the line of sight receiver location R8(69.0m, 25.0m).